Eur. Phys. J. B **51**, 75–78 (2006)
DOI: 10.1140/epjb/e2006-00194-9

THE EUROPEAN
PHYSICAL JOURNAL B

Electronic and optical properties of $Cd_{1-x}Zn_xS$ nanocrystals

N. Safta[1,a], A. Sakly[2], H. Mejri[1,3], and Y. Bouazra[2]

[1] Laboratoire de Physique des Semi-conducteurs et des Composants Électroniques, Faculté des Sciences, Avenue de l'environnement, 5000 Monastir, Tunisia
[2] Unité de Physique Quantique, Faculté des Sciences, Avenue de l'environnement, 5000 Monastir, Tunisia
[3] École Préparatoire aux Académies Militaires, Avenue Maréchal Tito, 4029 Sousse, Tunisia

Received 29 November 2005 / Received in final form 10 March 2006

Abstract. We report a numerical simulation of the conduction and valence band edges of $Cd_{1-x}Zn_xS$ nanocrystallites using a one — dimensional potential model. Electron — hole pairs are assumed to be confined in nanospheres of finite barrier heights. Optical absorption measurements are used to fit the bandgap of the $Cd_{1-x}Zn_xS$ nanocrystal material. A theoretical analysis is also made to calculate the energy location of bound excitons and the oscillator strength of interband transitions as a function of zinc composition. The aim of the latter study is to investigate the optical behavior of $Cd_{1-x}Zn_xS$ nanocrystals. An attempt to explain all the results is presented.

PACS. 73.21.La Quantum dots – 73.22.-f Electronic structure of nanoscale materials: clusters, nanoparticles, nanotubes, and nanocrystals – 71.55.Gs II-VI semiconductors

The study of structural and optical properties of nanocrystals is being one of the primary interests in both fundamental and applied research. Most studied are nanocrystals based on CdS [1]. It is well established that nanocrystalline compounds exhibit a quantum confinement effect [2–6] and show intermediate physical properties between the bulk solid and molecules as well. Depending on the crystalline size, two limiting confinements can occur. When the radius R of a nanocrystal is smaller than twice the exciton Bohr radius a_x, electrons and holes are considered as two confined particles bound by an enforced Coulomb interaction. However, for a crystalline semiconductor having R larger than $4a_x$, the ground exciton can be treated as a rigid quasiparticle. Thus, in nanocrystalites with relatively low radii, the motion of both electrons and holes as well as their energies are quantized, which leads to a widening in the band gap [1,7]. In the present work, our interest has been focused on $Cd_{1-x}Zn_xS$ nanocrystals with the aim to investigate their electronic and optical properties. It is to be noticed that the $Cd_{1-x}Zn_xS$ alloy is widely used as window layers for solar cells [7–15]. Despite the high potential of $Cd_{1-x}Zn_xS$ in device applications, this material has not been investigated further in nanocrystallites. More especially, the existing theoretical works seem to be insufficient to cover all the physical aspects of these nanostructures [7]. In this communication, we attempt to study theoretically the electro — optical properties of $Cd_{1-x}Zn_xS$ nanocrystals as a function of zinc composition. The paper is organized as follows: after a brief introduction, we present the computational method; in the following we report a modeling of $Cd_{1-x}Zn_xS$ nanocrystallites; conclusions are summarized in the last section.

As a system, we consider a pair of an electron and a hole, both confined in a spherical nanocrystallite of radius R. The semiconductor material is capped inside a dielectric matrix. For the $Cd_{1-x}Zn_xS$ system, sol-gel silica thin films were used as a surrounding dielectric host lattice to embedd the nanoparticles [7]. According to that reported in reference [16], only the electrons are assumed to be confined while the holes reside at the center of the nanospheres. More elaborate calculations have been made elsewhere, which consider the confinement of both free carriers [5,7,17]. It is worth noticing that the two approaches are based on an infinite potential barrier model. Here, we assume that both electrons and holes can undergo a quantum confinement and the boundary of the nanocrystallite is of finite barrier height. The latter assumption implies that free carriers can tunnel through the potential barrier. For a sake of simplicity, the electron and hole confinements are assumed to be uncorrelated. The Coulomb potential associated with the electron — hole interaction can be treated perturbavely or by using variational methods [18,19]. For the $Cd_{1-x}Zn_xS$ nanocrystal being investigated, the ground state of the electron — hole pair can be

---

[a] e-mail: `saftanabil@yahoo.fr`

described from the differential equations:

$$\left[-\frac{\hbar^2}{2m^*_{e,h}}\frac{1}{r_{e,h}}\frac{\partial^2}{\partial r^2_{e,h}}r_{e,h}+\frac{L^2_{e,h}}{2m^*_{e,h}r^2_{e,h}}\right.$$
$$\left.+V_{e,h}h\left(r_{e,h}-R\right)-\varepsilon_{e,h}\right]\Psi_{e,h}(r_{e,h})=0 \quad (1)$$

where $\hbar$ is the Plank's constant, m^* is the effective mass of the carriers, $\mathbf{L}$ represents the azimuthal momentum operator, V is the height of the confinement potential, $h(t)$ is the step function, ε is the confinement energy and $\psi\left(r\right)$ is the eigen wavefunction. The subscripts e and h refer to the electron and hole particles respectively. In deriving equation (1), we have used the effective mass theory and neglected the band nonparabolicity and the effective mass mismatch between the well and the barrier. Taking the eigenfunctions under the form

$$\Psi(r)=\frac{1}{r}\varphi(r)\,Y_l^m(\theta,\varphi)$$

where $Y_l^m\left(\theta,\varphi\right)$ are the spherical harmonics, equation (1) may be rewritten as:

$$\left[-\frac{\hbar^2}{2m^*_{e,h}}\frac{d^2}{dr^2_{e,h}}+\frac{l_{e,h}(l_{e,h}+1)\,\hbar^2}{2m^*_{e,h}r^2_{e,h}}\right.$$
$$\left.+V_{e,h}h\left(r_{e,h}-R\right)-\varepsilon_{e,h}\right]\varphi_{e,h}(r_{e,h})=0. \quad (2)$$

Here l denotes the quantum number associated with the operator $\mathbf{L}$. The function $\varphi(r)$ is subjected to be equal to zero at the center of the nanosphere. In the case of l different to zero, equation (2) can be solved by using the Bessel functions as an orthonormal basis set. However, for the bound states ns ($l = 0$), the problem to solve is reduced to a set of basic equations for an electron-hole pair in a one-dimensional potential well. In the following, we will restrict the study to these eigenstates. For energies such that $\varepsilon_{e,h} < V_{e,h}$, the wavefunctions should decay exponentially in the barrier. Thus, the confinement energies as well as the wavefunctions for the eigenstates ns in nanocrystals are given by:

$$\tan k_1 R+\frac{k_1}{k_2}=0 \quad (3)$$

and

$$\Psi_{e,h}(r_{e,h})=$$
$$\begin{cases}\dfrac{A_{e,h}}{r}\sin(k_{1e,h}r)\,Y_0^0\left(\theta,\varphi\right); & r\le R\\ \dfrac{A_{e,h}}{r}\sin(k_{1e,h}R)\,e^{k_{2e,h}(R-r)}Y_0^0\left(\theta,\varphi\right); & r\ge R\end{cases} \quad (4)$$

with

$$\hbar^2k^2_{1e,h}=2m^*_{e,h}\varepsilon_{e,h}$$
$$\hbar^2k^2_{2e,h}=2m^*_{e,h}\left(V_{e,h}-\varepsilon_{e,h}\right)$$

and

$$A_{e,h}=2^{\frac{1}{2}}\left[\pi R\left(1-\frac{\sin 2k_{1e,h}R}{2k_{1e,h}R}+\frac{\sin^2 k_{1e,h}R}{k_{2e,h}R}\right)\right]^{-\frac{1}{2}}$$

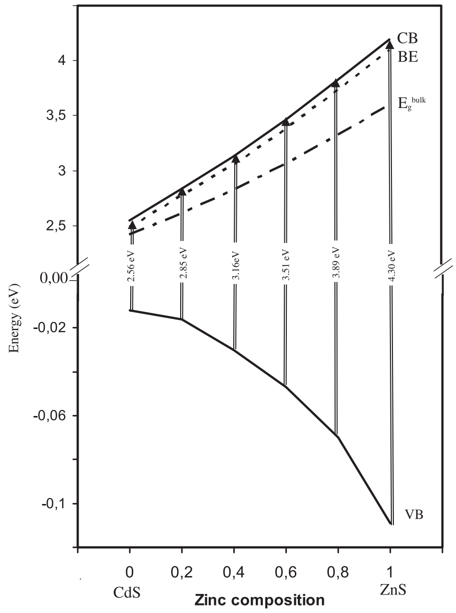

Fig. 1. The band gap energy as a function of x for $Cd_{1-x}Zn_xS$ quantum dots. CB and VB refer to the conduction and valence band edges. The energy emission of an interband transition is shown as a separation between the bands. The arrows indicate the absorption peak energies, as taken from reference [7]. Also reported in the plot are the band gap of bulk $Cd_{1-x}Zn_xS$ (in dashed line) and the energy position of the bound exciton state (in dotted line).

A is the normalized factor. In solving equation (3), V_e, V_h and R are treated as fitting parameters. If we now consider the electron-hole interaction, one has to solve for the ns bound states an exciton Hamiltonian in a square potential well (for solving this Hamiltonian see [18,19]).

With use of equation (3), we have calculated the conduction and valence band edges of a $Cd_{1-x}Zn_xS$ nanocrystal as a function of composition x. Results are depicted in Figure 1. As an experimental support, we have used absorption data obtained on $Cd_{1-x}Zn_xS$ thin films prepared by the sol-gel technique [7]. As can be noticed from the plot, the bandgap of the $Cd_{1-x}Zn_xS$ nanocrystalline material ranges from 2.56 to 4.30 eV, result in a good agreement with the relevant gap from optical absorption. The electron and hole effective masses used to calculate the subbands have been taken from references [1,20]. Values of these parameters and those of V_e, V_h and R are listed in Table 1. The change of the electron and hole effective masses as well as that of the relative dielectric constant in $Cd_{1-x}Zn_xS$ nanocrystallites with different zinc contents has been considered using linear interpolation. The zero energy is taken at the top of the valence bands of $Cd_{1-x}Zn_xS$ alloys. The dashed line is the plot of the bandgap versus x for bulk $Cd_{1-x}Zn_xS$ [21]. As also shown in Figure 1, both the conduction and valence bands are shifted in energy compared to the bulk due to the confinement of free carriers. The total energy shift is: $\Delta E_g=\varepsilon_e+\varepsilon_h$, which corresponds to the bandgap widening. As well demonstrated from the previous calculations,

Table 1. Parameters used to calculate the band edges for the $Cd_{1-x}Zn_xS$ nanocrystals.

x	m_e/m_0	m_{hh}/m_0	ε_r	V_e (eV)	V_h (eV)	R (nm)
0.0	0.20	5.00	8.5	0.13	0.13	2.0
0.2				0.40	0.10	2.0
0.4				0.40	0.20	1.5
0.6				1.00	1.00	1.5
0.8				1.25	1.00	1.3
1.0	0.28	1.76	8.0	01.75	0.60	1.2

the electron confinement energy shows a significant increase with the Zn molar fraction. This trend can be explained in terms of the x-dependence of the barrier potential. Indeed, the latter has been found to increase with increased Zn composition. In contrast, the hole confinement is not large going from CdS to ZnS, compared to that obtained for the electrons. To elucidate this behavior, it seems that the Cd substitution by a Zn atom induces a potential more attractive for the electrons. Also, the radius of the $Cd_{1-x}Zn_xS$ dots decreases as the Zn composition goes from zero to one. This can be explained by the fact that the crystalline sizes of $Cd_{1-x}Zn_xS$ decrease as x increases. (a(CdS) = 0.413; a(ZnS) = 0.381; c(CdS) = 0.676; c(ZnS)= 0.625 nm). Such a trend accentuates the confinement of free carriers in $Cd_{1-x}Zn_xS$ dots when increasing the zinc molar fraction. Let us now discuss the validity of the fitting parameters V_e, V_h and R. Concerning the two first ones, the previous works including reference [7] have considered them as infinite potential barriers for both electrons and holes. To our knowledge, there are no available data in the literature for comparison. As for the nanocrystallite size R, it has been however estimated using transmission electron micrograph measurements [7]. The particle radius is found to be of 4.5 and 2.0 nm for CdS and ZnS respectively [7]. For the intermediate Zn compositions, it was claimed in the same reference that the average of the nanocrystallite size of $Cd_{1-x}Zn_xS$ quantum dots varies between these two extreme values. The nanocrystallites size, as deduced from our calculations, does not show a significant discrepancy with respect to the relevant experimental values. There is an agreement in the order of magnitude of the two sets of particle size parameters. Most interesting, the same decreasing trend of the QD's crystalline size has been found in the two cases with increasing the ZnS molar fraction. $Cd_{1-x}Zn_xS$ quantum dots in borosilicate glass, on the other hand, have been investigated [22]. The average particle radius, as deduced from optical — absorption and Raman — scattering, is in the range 1.5–2.0 nm, which agree well with our nanocrystallites' sizes obtained. Using results of previous modeling, we have investigated excitonic properties in $Cd_{1-x}Zn_xS$ nanocrystallites as well. Calculations were made following Greene et al. [18]. The results obtained for the binding energy of bound-excitons (BE) are plotted in Figure 1. It is clearly seen that the energy of the exciton ground state increases with zinc composition. The following analytical law has been found to fit the exciton binding energy: $E_{exc}(x) = 0.0698 + 0.0364\,x + 0.0073\,x^2$ in eV. Concerning the increase of the exciton energy in nanocrystallites with different Zn compositions, it is most probably correlated to the x-dependence of the barrier heights that further confine free carriers as Zn content increases. On the other hand, a decrease in the dot radius when increasing x reduces the spatial exciton extension, giving rise to an increase in the energy of the exciton ground state. Also discussed in the paper is the efficiency of emission in $Cd_{1-x}Zn_xS$ nanocrystallites. According to the band gap results, the energy emission of interband transitions can be seen to vary in the 2.56 (484.1)–4.30 eV (288.2 nm) spectral range. This means that $Cd_{1-x}Zn_x$ S nanocrystals can emit in both ultraviolet and visible spectral wavelengths. Another characteristic of an electron transition is the oscillator strength [23]. For the $Cd_{1-x}Zn_xS$ system being studied, the oscillator strength of the ground interband transition is given by:

$$f_{CB\to VB} = \frac{2m_0}{\hbar^2}\left(E_g^{bulk} + \varepsilon_e + \varepsilon_h\right)\left|\langle\psi_e|\, r\, |\psi_h\rangle\right|^2 \qquad (5)$$

with

$$\begin{aligned}
\left|\langle\psi_e|\, r\, |\psi_h\rangle\right| = {} & \frac{1}{2\alpha^2}A_eA_h\left(\alpha R\sin\alpha R + \cos\alpha R - 1\right)\\
& - \frac{1}{2\beta^2}A_eA_h\left(\beta R\sin\beta R + \cos\beta R - 1\right)\\
& + \frac{1}{\gamma}A_eA_h\left(R + \frac{1}{\gamma}\right)\sin\frac{(\alpha+\beta)\,R}{2}\sin\frac{(\beta-\alpha)\,R}{2}
\end{aligned}$$

$$\begin{aligned}
\alpha &= k_{1e} - k_{1h}\\
\beta &= k_{1e} + k_{1h}\\
\gamma &= k_{2e} + k_{2h}
\end{aligned}$$

where m_0 is the free electron mass. We have calculated the x-dependent oscillator strength for the band-to-band transition using equation (5). Typical results, obtained for $R \sim 1.2$–2.0 nm, are shown in Figure 2. As has been found, the oscillator strength $f_{CB\to VB}$ first increases and then shows a decreasing tendency as x increases. Note that this decrease does not affect significantly the interband transition oscillator strengths. This means that the efficiency of radiative recombination in $Cd_{1-x}Zn_xS$ nanocrystallites is highly preserved.

In summary, we have investigated the electronic properties of $Cd_{1-x}Zn_xS$ nanocrystals. A particular attention has been paid to their compositional dependencies. Both electrons and holes are assumed to be confined in nanospheres with finite potential barriers at the boundary. By restricting the study to the bound ns states, the problem to solve is reduced to that of a one-dimensional potential well. Using this model, we have calculated the shape of the confining potentials, the quantized energies and their related envelope wave-functions. The theoretical results obtained for the x-dependent gap were fitted using optical absorption measurements. For the $Cd_{1-x}Zn_xS$ nanocrystals being studied, we have computed the binding energy of bound excitons and the oscillator strength of interband transitions as well. Calculations have been made

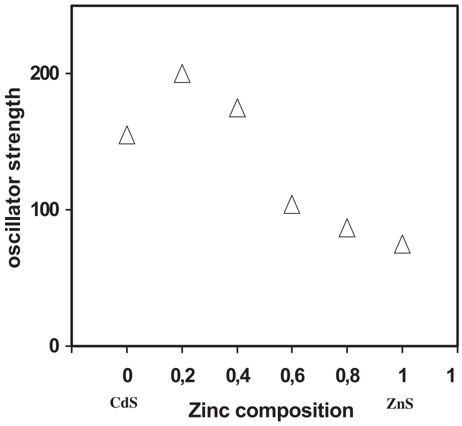

Fig. 2. The x-dependent oscillator strength of interband transitions in $Cd_{1-x}Zn_xS$ nanocrystals.

as a function of the ZnS molar fraction. A peculiar feature was revealed: $Cd_{1-x}Zn_xS$ dots can emit photon energies in the ultraviolet-visible spectral wavelength with relatively high efficiency. From a fundamental view point, a good understanding of the electronic and optical properties gives useful information on the free carrier distribution, the potential profile and the coupling between electron and hole gases within the nanocrystallites. In technological applications, this investigation is of great interest as well, more especially for designing devices based on II–VI and III–V nanocrystalline semiconductors.

References

1. K.K. Nanda, S.N. Sarangi, S. Mohanty, S.N. Sahu, Thin Solid Films **322**, 21 (1998)
2. Al.L. Efros, A.L. Efros, Sov. Phys. Semiconduc. **16**, 722 (1982)
3. L.E. Brus, J. Phys. Chem. **90**, 2555 (1986)
4. A. Schmitt-Rink, D.A.B. Miller, D.S. Chelma, Phys. Rev. B **35**, 8113 (1987)
5. Y. Kayanuma, Phys. Rev. B **38**, 7997 (1988)
6. L.E. Brus, Nanostruc. Mater. **1**, 71 (1992)
7. B. Bhattacharjee, S.K. Mandal, K. Chakrabarti, D. Ganguli, S. Chaudhui, J. Phys. D: Appl. Phys. **35**, 2636 (2002)
8. V. Alberts, R. Herberhonz, T. Walter, H.W. Scock, J. Phys. D: Appl. Phys. **30**, 2156 (1997)
9. N. Kohara, T. Negami, M. Nishitani, T. Wada, Jpn J. Appl. Phys **34**, L 1141
10. H.L. Kwok, J. Phys. D: Appl. Phys. **16**, 2367 (1983)
11. H.S. Kim, H.B. Im, J.T. Moon, Thin Solid Films **214**, 207 (1992)
12. G. Gordillo, Solar Energy Mater, Solar Cells **25**, 41 (1992)
13. J.W. Bowron, S.D. Damaskinos, A.E. Dixon, Solar cells **31**, 159 (1991)
14. O.M. Hussain, P.S. Reddy, B.S. Naidu, U. Uthanna, P.J. Reddy, Semicond. Sci. Technol. **6**, 690 (1991)
15. T.L. Chu, S.S. Chu, J. Britt, C. Feredikes, C.Q. Wu, J. Appl. Phys. **70**, 2688 (1991)
16. M.C. Klein, F. Hache, D. Ricard, C. Flytzanis, Phys. Rev. B **42**, 11123 (1990)
17. A.L. Efros, Sov. Phys. Semicond **16**, 772 (1992)
18. R.L. Greene, K.K. Bajaj, Solid State Commun. **45**, 831 (1983); R.L. Greene, K.K. Bajaj, D.E. Phelps, Phys. Rev. B **29**, 1807 (1984)
19. G. Bastard, E.E. Mendez, L.L. Chang, L. Esaki, Phys. Rev. B **26**, 1974 (1982)
20. H. Mathieu, *Physique des semi-conducteurs et des composants électroniques* (Masson, Paris, 1987, 1990)
21. G.K. Padam, G.L. Mahotra, S.U.M. Rao, J. Appl. Phys. **63**, 770 (1988)
22. H. Yükselici, P.D. Persans, T.M. Hayes, Phys. Rev. B **52**, 11763 (1995)
23. W.Q. Chen, T.G. Andersson, J. Appl. Phys. **73**, 4484 (1993)